Synthesis and Characterization of Highly Magnetized Nanocrystalline $Co_{30}Fe_{70}$ Alloy by Chemical Reduction

Chang Woo Kim,[†] Young Hwan Kim,[†] Hyun Gil Cha,[†] Hae Woong Kwon,[‡] and Young Soo Kang*,[†]

Department of Chemistry, Pukyong National University, Busan 608-737, Korea, and School of Materials Science and Engineering, Pukyong National University, Busan 608-739, Korea

Received: July 13, 2006; In Final Form: September 1, 2006

$Co_{30}Fe_{70}$ nanoparticles with mean particle size of about 8 nm were successfully synthesized by the chemical reduction of cobalt chloride and iron chloride with borohydride as a reducing agent in aqueous solution. The composition and size of the $Co_{30}Fe_{70}$ nanoparticles were optimized by controlling the molar ratio of starting materials, reaction time, and dropping rate of aqueous reducing agent. As alloy powders prepared by chemical reduction tend to be amorphous in the as-synthesized state, the as-precipitated $Co_{30}Fe_{70}$ nanoparticles were heat-treated to achieve crystallinity at the different temperatures for 1 h. The $Co_{30}Fe_{70}$ nanocrystallite by chemical reduction shows excellent soft magnetic behavior, such as high permeability, negligible coercivity, and high saturation magnetization like that of $Co_{30}Fe_{70}$ bulk.

Introduction

Nanocomposite permanent magnets can exhibit a very high maximum energy product ($(BH)_{max}$) due to the high moment (M_s) of the soft phase and the large coercivity (H_c) of the hard phase.[1,2] Most of the exchange coupled permanent magnets such as $Nd_2Fe_{14}B/Fe_3B$ and $Nd_2Fe_{14}B/\alpha$-Fe reported nowadays have been prepared by annealing melt-spun ribbons, mechanically milled alloys, HDDR, and so forth, since the seminal work of Hadjipanayis and his colleagues.[3,4] The microstructure obtained in these cases was not very uniform, and the grain size of the soft phase tended to be too large for maximum exchange coupling.[5−10] In such a system, a critical factor in fabricating a permanent magnet having an efficient exchange coupling effect is the grain size of the crystalline soft phase, which should be smaller than 20 nm for efficient 3D alignment at 800 °C, the annealing temperature to fabricate bulk magnets.[11,12] Second, interaction between the hard and soft magnetic grains cannot be successfully obtained in the presence of impurities such as surfactant or stabilizer.[13]

As one of the best soft magnetic materials, the Co−Fe alloys exhibit the high saturation magnetization, M_s, and the high curie temperature, T_c ($T_c \approx 900$ °C), that make them potential candidates for the high-temperature applications.[14] It is well-known that Co and Fe form the body-centered-cubic solid solution (Co_xFe_{100-x}) over an extensive range.[15] In the range $30 < x < 70$, Co−Fe alloys undergo a phase transformation from a disordered body-centered-cubic structure to the ordered CsCl type structure below 730 °C. The ordered Co−Fe alloys are excellent soft magnetic materials with negligible magnetocrystalline anisotropy, K_1. As the magnetic stability of individual particle scales with the anisotropy constant, the particle volume, small Co−Fe particles may be suitable for future ultra-high-density magnetic recording media and for use in electric vehicles and other applications operating at high temperature. Until this time, the synthesis of Co−Fe nanoparticle has mainly relied on vacuum deposition techniques. Postdeposition annealing and random nucleation in the initial stages of growth, however, typically results in broad distributions of particle sizes, which may be further aggravated by agglomeration during annealing.

Solution-phase chemical synthesis reported by Murphy et al.[16,17] has been successfully used to prepare monodisperse metal nanoparticles with the unique magnetic, electric, and mechanical properties derived from small particle sizes and uniform size distribution, compared to physically prepared magnetic materials.[18−24] Specially, in the case of the soft magnetic materials, Sun et al. have prepared spherical FePt nanoparticles with a very narrow size distribution that are superparamagnetic.[25] More recently, Alivisatos and co-workers[26] have reported an extremely interesting Co system with high crystallinity, narrow size distributions, and a high degree of shape control.[27] However, synthetic procedures have not yet been developed to prepare monodisperse soft magnetic $Co_{30}Fe_{70}$ nanoparticles so far. Moreover, most of the studies on magnetic nanoparticle have only focused on the synthesis of uniform spherical forms and the control of their particle size, and their magnetic properties are substantially low as compared with bulk material for permanent magnets. This point can be the best advantage for magnetic storage media, sensors, and ferrofluids, and so forth, but acts as a disadvantage for permanent magnetic materials or advanced permanent magnet applications. Thus, the breakthrough in the enhancement of magnetic properties is an important development and achievement.

We have reported on the chemical synthesis of monodisperse Co- and Fe-based nanoparticle as soft magnetic phase with controlled size and shape by Langmuir−Blodgett technique,[28] M^{2+}-oleate$_2$,[13] and chemical reduction.[29] Here, we first report nanocrystalline $Co_{30}Fe_{70}$ alloy by chemical reduction as soft magnetic material. Chemical reduction synthesis reported in this study is a comparatively inexpensive and easy way to produce nanoparticles with highly controllable size and morphology.[30]

* Address correspondence to this author. Tel.: + 82 51 510 6379. Fax.: + 82 51 581 8147. E-mail: yskang@pknu.ac.kr.
[†] Department of Chemistry.
[‡] School of Materials Science and Engineering.

10.1021/jp064440+ CCC: $33.50
Published on Web 11/02/2006

In addition, we have obtained the magnetic soft-phase $Co_{30}Fe_{70}$ alloy with the bulklike magnetic property through optimum annealing time and temperature. Moreover, the chemical reduction synthesis is free from surfactant or stabilizer which was used by the polyol process,[31] the thermal decomposition method,[32] and so on. In this point of view, nanocrystalline $Co_{30}Fe_{70}$ alloy by the chemical reduction synthesis in this work can be efficiently used as a good soft magnetic material with bulklike magnetic property.

Experimental Section

Synthesis of $Co_{30}Fe_{70}$ Alloys. Cobalt chloride hexahydrate ($CoCl_2 \cdot 6H_2O$, 98%), iron chloride tetrahydrate ($FeCl_2 \cdot 4H_2O$, 99+%), and sodium borohydride ($NaBH_4$) were purchased from Aldrich. High-purity Ar gas (99.999+%) was used to prevent oxidation during purging the distilled water and drying the synthesized nanoparticles. The reactor, having two inlets for borohydride solution and high-purity Ar gas and one outlet for exhaust for free hydrogen gas, was fitted with a magnetic stirrer. In a 250 mL three-necked round-bottom flask under an argon atmosphere, $CoCl_2 \cdot 6H_2O$ (0.002 mol, 0.7716 g) and $FeCl_2 \cdot 4H_2O$ (0.008 mol, 1.5261 g) were dissolved in 50 mL deoxygenated water by magnetic stirring. A 50 mL aliquot of 0.12 M $NaBH_4$ (0.006 mol, 0.2269 g) was dropped into the metal solution with vigorous stirring. The drop of aqueous $NaBH_4$ was put into the metal solution at a dropping rate of 0.5 mL/s at room temperature. The overall reaction time was kept for 3 min. As the reaction was processed, the very fine metallic powder was formed. The resultant black precipitate was washed with deoxygenated water in order to remove the reaction residues and acetone to get rid of deoxygenated water. After the acetone−wet powders were dried in the furnace with a slow flow of argon gas at room temperature, as-synthesized $Co_{30}Fe_{70}$ nanoparticles were put into isooctane with oleic acid, and then, isooctane solution was dispersed with ultrasonic agitation for 1 h. $Co_{30}Fe_{70}$ nanoparticles for TEM imaging were formed by self-assembly when a drop of nanoparticles in isooctane solution was carefully placed on the Cu grid and dried in air. As-synthesized Co−Fe alloy was annealed at 400 °C and at 800 °C with at a heating rate of 7 °C per min in a vacuum system with 2×10^{-5} mbar. The products were stored in an organic solvent. All the processes were performed in the glovebox with an atmosphere of high-purity argon gas.

Characterization. To identify the properties of the prepared $Co_{30}Fe_{70}$ nanoparticles, we did various experiments. Elemental analyses were conducted by using electron probe X-ray microanalysis (EPMA-1600, Shimadzu, Japan), inductively coupled plasma spectroscopy (ICP), and energy-dispersive X-ray microanalysis (EDX) with JEOL JEM2010 TEM operated under an acceleration voltage of 200 kV. The surface morphology of nanoparticles was confirmed with field emission scanning electron microscopy (FE-SEM). FE-SEM measurement was carried out on JEOL LTD JSM 890. The size and shape of nanoparticles were investigated by transmission electron microscopy (TEM). TEM measurements were carried out on a Hitachi H-7500 (low resolution) and JEOL JEM2010 (high resolution) TEM. The size distribution of the particles was measured from enlarged photographs of TEM images. The as-synthesized precipitate was analyzed by differential thermal analysis (DTA) to investigate the crystallization temperature of the precipitate. The crystal structure of the as-annealed nanoparticles was identified by using X-ray powder diffraction (XRD) with a Philips X'Pert-MPD System using monochromated a Cu−Kα radiation source ($\lambda = 0.154\,056$ nm). After the powder sample was set with wax to prevent physical rotation of the particles, the magnetic properties were measured by Lake Shore 7300 vibrating sample magnetometer (VSM) with applied field up to 15 kOe and with a superconducting quantum interference device (SQUID) magnetometer (Quantum Design, MPMS XL 7) in a maximum field of 7 T.

Results and Discussion

Structure Analyses. Chemical reduction involves the simultaneous occurrence of nucleation, growth, coarsening, and/or agglomeration processes.[33] The products of chemical reduction are generally sparingly soluble species formed under conditions of high supersaturation. Such conditions dictate that nucleation will be a key step of the precipitation process and that a large number of small particles will be formed.[34] As such, any reaction conditions influencing the reaction procedure, such as concentration, BH_4^-/M ion ratio, and pH, must be considered to be relevant to product identity, morphology, particle size, and particle size distribution.[35] It is well-known that boron is incorporated into the solid products, and the metal/boron ratios vary widely according to literature report.[36] In aqueous solution under anaerobic conditions, the reaction of metal ions with borohydride gives finely divided black precipitates of metals and metal boride.[37] Depending upon the concentration of reactants, the borohydride reaction generally follows one of the following chemical paths:

$$BH_4^- + 2M^{2+} + 2H_2O = 2M\downarrow + BO_2^- + 4H^+ + 2H_2\uparrow \quad (1)$$

$$2BH_4^- + 2M^{2+} + 2H_2O = M_2B\downarrow + HBO_2^- + 2H^+ + 4.5H_2\uparrow \quad (2)$$

The synthesis conditions have been optimized for the reaction that follows as in eq 1 to obtain boron-free nanosized metallic alloy. The borohydride solution reacts exothermally to the metal salt solutions, and a large amount of heat is generated in the reactor. The amount of generated heat is sufficient to cause the oxidation of the nanosized metal alloy; therefore, during the reaction the solution was stirred vigorously to dissipate heat to surroundings. Hence, reaction conditions were controlled with the BH_4^-/M ion ratio and by dropping reducing agent at ambient temperature in order to avoid the formation of metal borides. The molar ratio of BH_4^- to M for equivalent reactions is around 0.5:1.0. This method is very simple, and kinetics is so controlled as to prefer particle nucleation over particle growth and to yield ultrafine metallic powder. As shown in Figure 1, X-ray data shows that the ratio of Co to Fe is around 30:70 in the prepared precipitate. This result was in good agreement with that of EDX and ICP. It means that no impure element such as B was contained in the precipitate. It was interesting to note that no boron trace was found in the powder. Boron and other byproducts were found to be present in the filtrate. FE-SEM image shows that acicular $Co_{30}Fe_{70}$ particles agglomerated into larger particles without regular shape. To know the mean particle size exactly, the size and shape of as-synthesized particles were investigated by TEM. Figure 2 shows TEM image (a), ED pattern (b), EDX spectrum (c), and histogram of size distribution (d) of as-synthesized $Co_{30}Fe_{70}$ nanoparticles by chemical reduction. This indicates that FE-SEM and TEM images of the as-prepared powders revealed chainlike aggregates of 8−10 nm $Co_{30}Fe_{70}$ alloy. Dipole−dipole interactions between single particles have caused formation of acicular-like chains up to micrometer-scale length. As can be seen in ED pattern and EDX

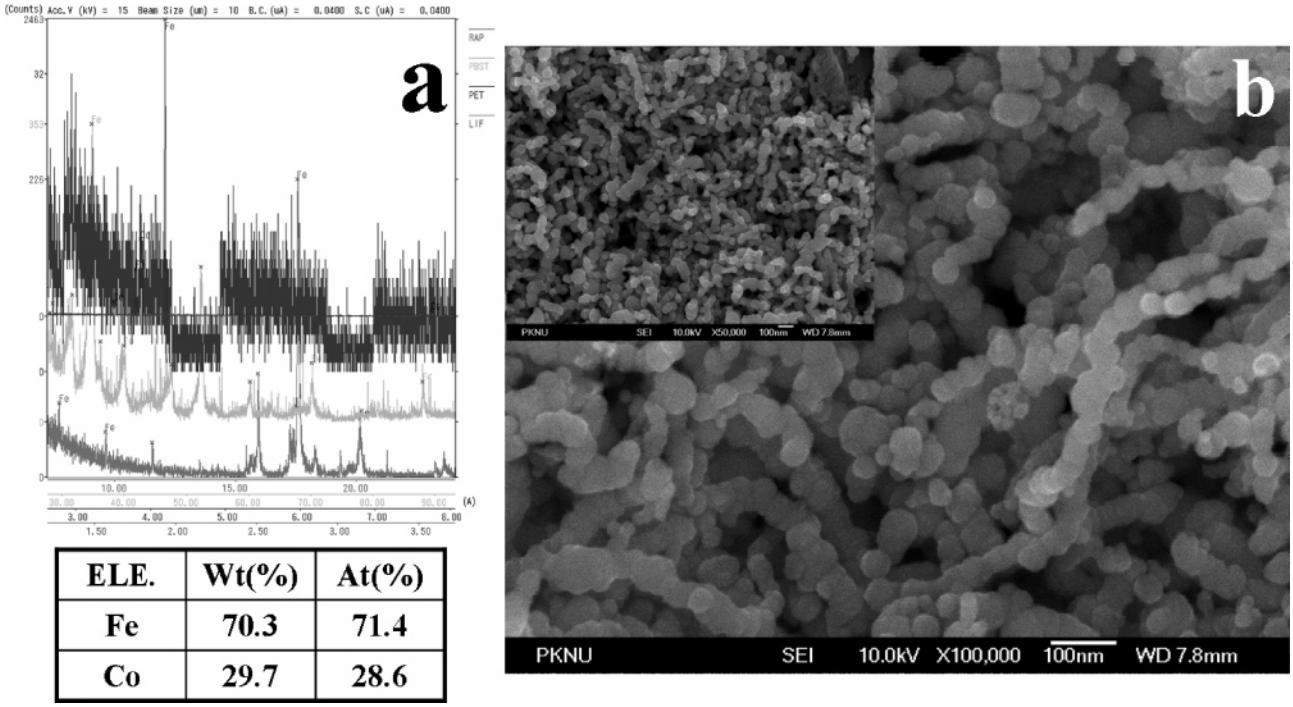

ELE.	Wt(%)	At(%)
Fe	70.3	71.4
Co	29.7	28.6

Figure 1. EPMA spectrum (a) and FE-SEM image (b) of as-synthesized Co−Fe alloy by chemical reduction.

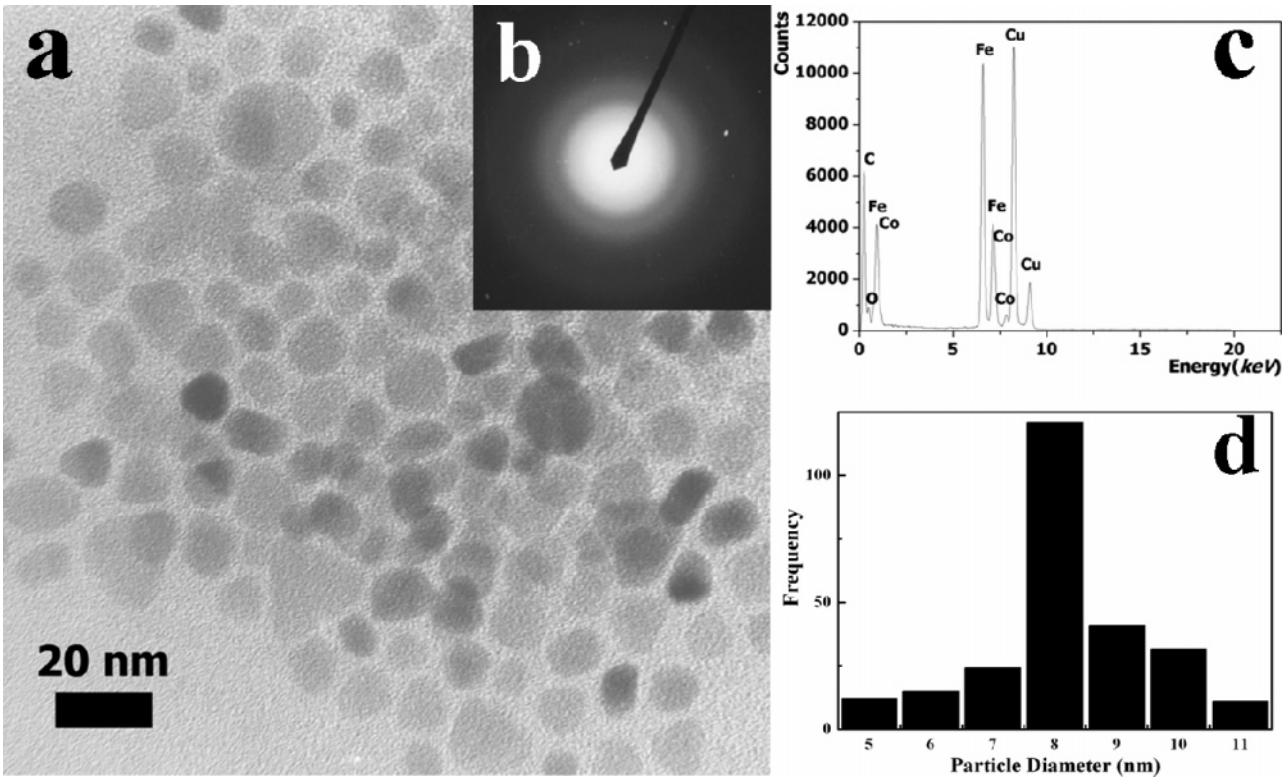

Figure 2. TEM image (a), electron-diffraction pattern (b), EDX spectrum (c), and histogram of size distribution (d) of as-synthesized Co−Fe alloy nanoparticle by chemical reduction.

spectrum of Figure 2, the broad and diffuse Debye rings in the image of as-precipitated nanoparticles which are only composed of Co and Fe indicate the amorphous structure of the sample, in a good agreement not only with that reported in the literature but also with that of $Co_{30}Fe_{70}$ alloy detected by XRD in Figure 4.[38] The amorphous phase is formed because the chemical reaction takes place below the glass transition temperature.[39] Figure 3 shows DTA and TGA curves of the synthesized Co_{30}-Fe_{70} nanoparticle, which were collected at a heating rate of 7 °C per 1 min, with the sample kept under high-purity argon atmosphere. The DTA thermogram of the as-synthesized Co_{30}-Fe_{70} alloy has two exotherms at 340 °C and at 450 °C. The first exotherm at 340 °C may be attributed to an amorphous-to-crystalline transition in the sample. The second exotherm at 450 °C may be due to subsequent bonding and coarsening of crystalline particles. Because alloy powders made by chemical reduction tend to be amorphous in the as-synthesized state, the as-prepared amorphous $Co_{30}Fe_{70}$ nanoparticles were heat-treated

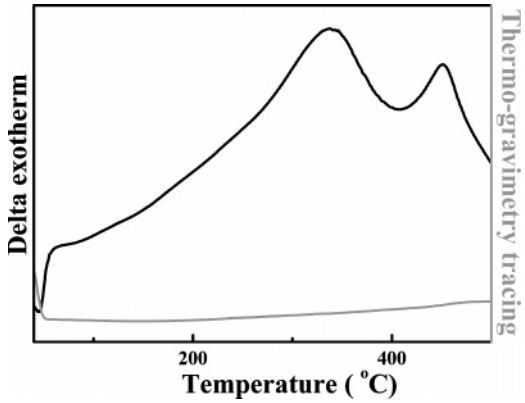

Figure 3. DTA thermogram and TGA curve of as-synthesized Co−Fe alloy.

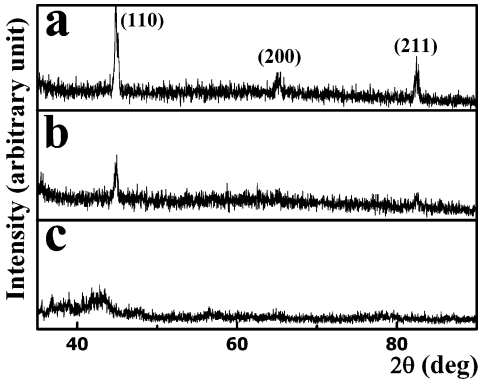

Figure 4. XRD spectra of the nanocrystallite $Co_{30}Fe_{70}$ alloy annealed at 800 °C (a), as-annealed at 400 °C (b) for 1 h, and as-synthesized Co−Fe alloy (c).

to achieve crystallinity at the different temperatures for 1 h, respectively. Thus, the as-synthesized $Co_{30}Fe_{70}$ alloy was heat-treated at 400 °C (in Figure 4b), which is lower than bonding and coarsening temperature, and at 800 °C (in Figure 4a), which is a phase transition temperature with a heating rate of 7 °C per min in a vacuum system at 2×10^{-5} mbar, and then was kept for 1 h, respectively. The crystalline structure of $Co_{30}Fe_{70}$ fine particles was characterized using X-ray diffractometer. Figure 4 shows that the XRD pattern contained broad features centered on the positions for the strongest reflections of the expected solid solution phase in the case of the as-synthesized $Co_{30}Fe_{70}$ alloy (Figure 4c). It suggests that amorphous Co_{30}-Fe_{70} alloy is the primary constituent of the as-precipitated powders forming solid solution. Figure 4a shows that there are peaks at $2\theta = 44.8°$, 65.0°, and 82.5°, which reveal the presence of a BCC crystalline structure with lattice constant $\alpha = 2.863$ Å. The discernible peaks can be indexed to (110), (200), and (211) planes of a cubic unit cell, which correspond to cubic structure of $Co_{30}Fe_{70}$. This is in good agreement with the structure of a BCC Co_3Fe_7 alloy in JCPDS card (no. 48-1816). The crystal sizes of the Co−Fe alloys in Figure 4a,b determined by the Debye−Scherrer equation with XRD data are 19.5 and 15.2 nm, respectively. Figure 5 shows TEM images (a) with different magnitudes, EDX spectrum (b), and histogram of size distribution (c) of $Co_{30}Fe_{70}$ alloy which was heat-treated at 400 °C for 1 h in a vacuum system at 2×10^{-5} mbar. As can be seen in TEM images, the size of the $Co_{30}Fe_{70}$ nanoparticles was determined to be around 9−12 nm. It is close to the particle size which was calculated by the Debye−Scherrer equation with the XRD data in Figure 4. It means that an amorphous-to-crystalline transition occurs without particle size growth, compared with that of as-synthesized $Co_{30}Fe_{70}$ nanoparticles, because the amorphous $Co_{30}Fe_{70}$ alloy was heat-treated at 400 °C, lower than the bonding and coarsening temperature as shown in the DTA thermogram. Figure 6 shows TEM images (a) with different magnitudes, ED pattern (b), and histogram of size distribution (c) of $Co_{30}Fe_{70}$ nanocrystallite which was heat-treated at 800 °C for 1 h. Most of the $Co_{30}Fe_{70}$ nanocrystallite consisted of 16-nm particles that are spherical and well-aligned

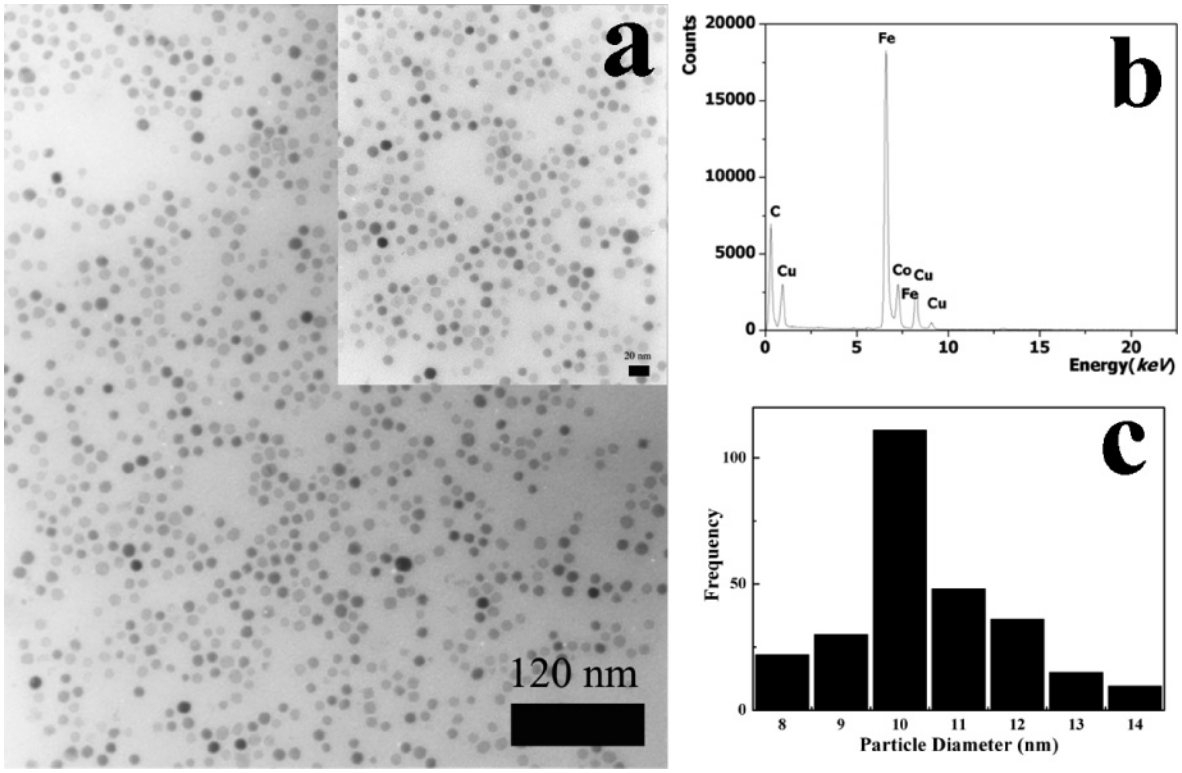

Figure 5. TEM images (a), EDX spectrum (b), and histogram of size distribution (c) of $Co_{30}Fe_{70}$ alloy which was annealed at 400 °C for 1 h.

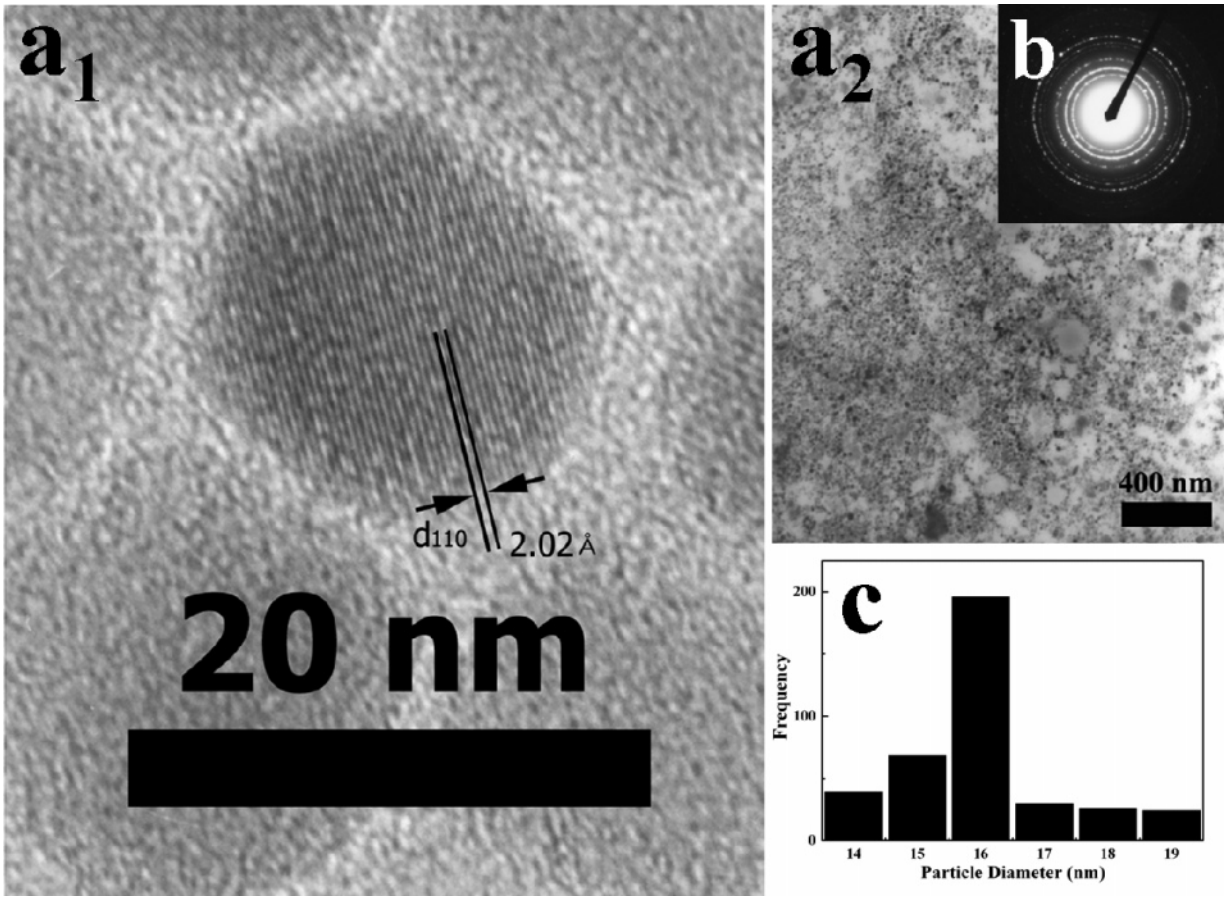

Figure 6. HR-TEM images (a) with different magnitudes, electron-diffraction pattern (b), and histogram of size distribution (c) of $Co_{30}Fe_{70}$ nanocrystallite which was annealed at 800 °C for 1 h.

vertically, which is close to the particle sizes calculated from Debye−Scherrer equation with XRD data. The lattice spacing of $Co_{30}Fe_{70}$ nanocrystallite is 2.02 Å, which is consistent with the lattice spacing of (110) plane of the Co_3Fe_7 crystal structure (JCPDS card, no. 48-1816). The Co−Fe phase undergoes disorder−order transition when heated to around 800 °C. The B2 structure ($CsCl_2$) of Co−Fe alloy is an ordered BCC structure and can be viewed as two interpenetrating simple cubic sublattices in which Fe atom occupies one sublattice and Co atom occupies the other sublattice. Therefore, it is concluded that Co atoms have occupied Fe atomic sites in the BCC structure.

Magnetic Properties. As-synthesized $Co_{30}Fe_{70}$ alloy and $Co_{30}Fe_{70}$ nanocrystallites which were heat-treated at 400 °C and at 800 °C for 1 h were investigated by VSM with applied field up to 15 kOe at 300 K. Figure 7 shows the magnetization curve of $Co_{30}Fe_{70}$ nanoparticles annealed at 800 °C (a), at 400 °C (b) for 1 h, and as-synthesized alloy (c). As can be seen in Figure 7, the value of magnetization (M) of the as-made $Co_{30}Fe_{70}$ nanoparticles (c) is 147.8 emu/g with applied field of 15 kOe, because the as-made $Co_{30}Fe_{70}$ is amorphous phase and the crystallinity is weak. However, M of the as-annealed $Co_{30}Fe_{70}$ nanocrystallite is getting larger as the crystallinity increases. In the case of $Co_{30}Fe_{70}$ nanocrystallite (a) which was annealed at 800 °C for 1 h, it can be expected that M_s of $Co_{30}Fe_{70}$ nanocrystallite is over 210.5 emu/g because M of $Co_{30}Fe_{70}$ nanocrystallite was not fully saturated with an applied field of 15 kOe. The as-annealed $Co_{30}Fe_{70}$ alloy was measured by SQUID in a maximum field of 7 T at room temperature. Figure 8 shows that M of $Co_{30}Fe_{70}$ nanocrystallite was nearly saturated with an applied field of 4 T. As can be seen in Figures 7 and

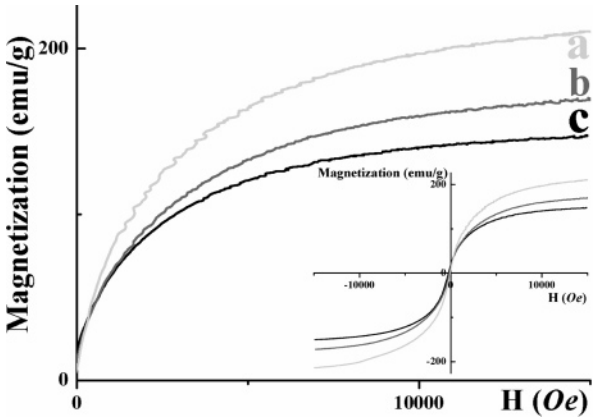

Figure 7. Magnetization curve of $Co_{30}Fe_{70}$ nanocrystallite which was annealed at 800 °C (a), and at 400 °C (b) for 1 h, and as-synthesized $Co_{30}Fe_{70}$ alloy (c).

8, there is almost negligible coercivity (<50 Oe) and M_s of $Co_{30}Fe_{70}$ nanocrystallite is 225.4 emu/g with SQUID in a maximum field of 7 T at room temperature. Figure 9 shows magnetization (emu/g) by VSM results and the particle size (nm) by Debye−Scherrer equation with XRD data of $Co_{30}Fe_{70}$ alloy according to annealing temperature under inert atmosphere for 1 h. It is important to mention not only that M_s of $Co_{30}Fe_{70}$ nanocrystallite by chemical reduction synthesis exceeds M_s of Fe bulk (M_s = 215 emu/g in the literature) but also that the $Co_{30}Fe_{70}$ nanocrystallite has a value of M_s similar to that of bulk (M_s = 230 emu/g in the literature). It means that saturation magnetization of Fe increases with Co addition because of increasing polarization of Fe atoms with Co additions. In addition, the size of as-

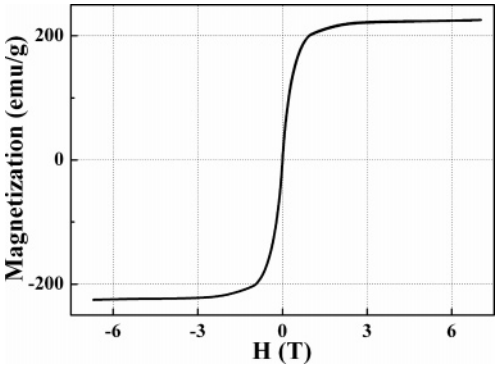

Figure 8. Hysteresis loop of the $Co_{30}Fe_{70}$ nanocrystallite which was annealed at 800 °C for 1 h.

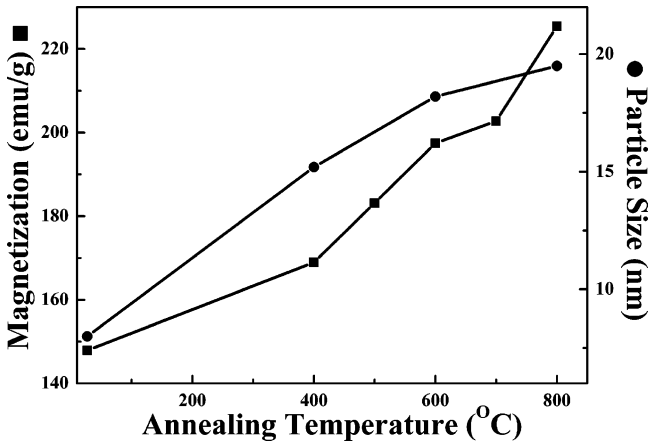

Figure 9. Magnetization (■) and particle size (●) of $Co_{30}Fe_{70}$ alloy.

made $Co_{30}Fe_{70}$ nanoparticles by chemical reduction is even smaller than 20 nm and did not particularly get larger even after the amorphous $Co_{30}Fe_{70}$ nanoparticle was annealed at 800 °C for 1 h. Accordingly, this value with the nanosized particles is the highest M_s value of the powder which has ever been synthesized by the thermal decomposition method or any other chemical method. Last, the loop shape in Figures 7 and 8 may show superparamagnetic behavior at room temperature. Further measurements are necessary to determine whether the $Co_{30}Fe_{70}$ nanocrystallite with 16-nm size shows superparamagnetic behavior.

Conclusion

In summary, among various techniques to produce nanocrystalline magnetic materials, the chemical reduction synthesis is a good and easy treatment to get uniform and spherical nanosized particles without component change or other contamination, and kinetics is so controlled as to prefer particle nucleation over particle growth and to yield ultrafine metallic powder. Moreover, the method may be used for the large-scale production of ultrafine amorphous alloy particles. In this point of view, $Co_{30}Fe_{70}$ nanocrystallite by the chemical reduction method shows excellent soft magnetic behavior, such as high permeability, negligible coercivity, and high saturation magnetization like that of $Co_{30}Fe_{70}$ bulk. Finally, the chemical reduction method may be employed to obtain nanopowders of Co−Fe alloys, and powder processing approaches combined with chemical reduction may pave the way for significantly superior soft magnetic products for the 21st century and beyond.

Acknowledgment. This work was supported by the Korean National Research Laboratory Program. We would like to thank financial support by the Brain Korea 21 project in 2006.

Supporting Information Available: TMA curve of nanocrystallite $Co_{30}Fe_{70}$ alloy. This material is available free of charge via the Internet at http://pubs.acs.org.

References and Notes

(1) Hadjipanayis, G. C. *J. Magn. Magn. Mater.* **1999**, *200*, 373.
(2) Chen, Z.; Zhang, Y.; Hadjipanayis, G. C.; Chen, Q.; Ma, B. *J. Alloys Compd.* **1999**, *287*, 227.
(3) Liu, S.; Hilton, S.; Zhang, Y.; Hadjipanayis, G.; Chen, C.; Lee, D. *INTERMAG 2003 of the 2003 IEEE International Magnetics Conference.* 2003, EB-07.
(4) Chen, Z.; Zhang, Y.; Hadjipanayis, G. C.; Chen, Q.; Ma, B. *J. Alloys Compd.* **1999**, *287*, 227.
(5) Yan, A.; Bollero, A.; Gutfleisch, O.; Muller, K.-H. *J. Phys. D: Appl. Phys.* **2002**, *35*, 835.
(6) David, S.; Givord, D. *J. Alloys Compd.* **1998**, *281*, 6.
(7) Goll, D., Seeger, M.; Kronmuller, H. *J. Magn. Magn. Mater.* **1998**, *185*, 49.
(8) Lewis, L. H.; Moodenbaugh, A. R.; Welch, D. O.; Panchanathan, V. *J. Phys. D: Appl. Phys.* **2001**, *34*, 744.
(9) Zhang, H.; Sun, Z.; Zhang, S.; Han, B.; Shen, B. *Phys. Rev. B* **2002**, *60*, 64.
(10) Kneller, E. F.; Hawig, R. *IEEE Trans. Magn.* **1991**, *27*, 3588.
(11) Fischer, R.; Schrefl, T.; Kronmuller, H. *J. Magn. Magn. Mater.* **1996**, *153*, 35.
(12) Skomski, R.; Coey, J. M. D. *Phys. Rev. B* **1993**, *48*, 15812.
(13) Lee, D. K.; Kim, Y. H.; Zhang, X.; Kang, Y. S. *Curr. Appl. Phys.* **2006**, *6*, 786.
(14) Li, L. *J. Appl. Phys.* **1996**, *79*, 4578.
(15) Sourmail, T. *Prog. Mater. Sci.* **2005**, *50*, 816.
(16) Mallin, M. P.; Murph, C. J. *Nano Lett.* **2002**, *2* (11), 1235.
(17) Gou, L.; Murph, C. J. *Nano Lett.* **2003**, *3*, 231.
(18) Zeng, H.; Li, J.; Wang, J. L.; Liu, J. P.; Sun, S. *Nano Lett.* **2004**, *4*, 187.
(19) Song, H.; Kim, F.; Connor, S.; Somorjai, G. A.; Yang, P. *J. Phys. Chem. B* **2005**, *109*, 188.
(20) Yu, H.; Gibbons, P. C.; Kelton, K. F.; Buhro, W. E. *J. Am. Chem. Soc.* **2001**, *123*, 9198.
(21) Lu, Y.; Yin, Y.; Myers, B. T.; Xia, Y *Nano Lett.* **2002**, *2*, 183.
(22) Lee, D. K.; Kang, Y. S. *Colloids Surf., A* **2005**, *257*−*258*, 237.
(23) Li, J.; Zeng, H.; Sun, S.; Liu, J. P.; Wang, Z. L. *J. Phys. Chem. B* **2004**, *108*, 14005.
(24) Sobal, N. S.; Ebel, U.; Mohwald, H.; Giersig, M. *J. Phys. Chem. B* **2003**, *107*, 7351.
(25) Sun, S.; Murray, C. B.; Weller, D.; Folks, L.; Moser, A. *Science* **2000**, *287*, 1989.
(26) Puntes, V. F.; Krishnan, K. M.; Alivisatos, A. P. *Science* **2001**, *291*, 2115.
(27) Puntes, V. F.; Zanchet, D.; Erdonmez, C. K.; Alivisatos, A. P. *J. Am. Chem. Soc.* **2002**, *124*, 12874.
(28) Lee, D. K.; Kim, Y. H.; Kang, Y. S.; Stroeve, P. *J. Phys. Chem. B* **2005**, *109*, 14939.
(29) Kim, C. W.; Kim, Y. H.; Lee, D. K.; Cha, H. G.; Kang, Y. S. *J. Nanosci. Nanotechnol.* **2006**, in press.
(30) Zheng, Q.; Zhang, Y.; Wang, H. L.; Papaefthymiou, V.; Hadjipanayis, G. C. *J. Magn. Magn. Mater.* **2004**, 272−276, E1223.
(31) Fivet, F.; Lagier, J. P.; Figlarz, M. *MRS Bull.* **1989**, *14*, 29.
(32) Park, S.-J.; Kim, S.; Lee, S.; Khim, Z. G.; Char, K.; Hyeon, T. *J. Am. Chem. Soc.* **2000**, *122*, 8581.
(33) Cushing, B. L.; Kolesnichenko, V. L.; O'Connor, C. J. *Chem. Rev.* **2004**, *104*, 3893.
(34) Gleeve, G. N.; Klabunde, K. J.; Sorensen, C. M.; Hadjipanayis, G. C. *Inorg. Chem.* **1995**, *34*, 28.
(35) Gleeve, G. N.; Klabunde, K. J.; Sorensen, C. M.; Hadjipanayis, G. C. *Langmuir* **1994**, *10*, 4726.
(36) Gleeve, G. N.; Klabunde, K. J.; Sorensen, C. M.; Hadjipanayis, G. C. *Langmuir* **1993**, *9*, 162.
(37) Jana, N. R.; Gearheart, L.; Murphy, C. J. *Chem. Mater.* **2001**, *13*, 2313.
(38) Harber, J. A.; Gunda, N. V.; Balbach, J. J.; Conradi, M. S.; Buhro, W. E. *Chem. Mater.* **2000**, *12*, 973.
(39) Shen, J.; Li, Z.; Yan, Q.; Chen, Y. *J. Phys. Chem.* **1993**, *97*, 8504.